Structural Engineering and Mechanics, *Vol. 50, No. 2 (2014) 181-199*
DOI: http://dx.doi.org/10.12989/sem.2014.50.2.181

Is it shear locking or mesh refinement problem?

Y.I. Özdemir[*1] and Y. Ayvaz[2a]

[1]*Department of Civil Engineering, Karadeniz Technical University, Trabzon, Turkey*
[2]*Civil Enginnering Department,Yıldız Technical University, İstanbul, Turkey*

(Received July 5, 2012, Revised February 8, 2014, Accepted February 25, 2014)

Abstract. Locking phenomenon is a mesh problem and can be staved off with mesh refinement. If the studier is not preferred going to the solution with increasing mesh size or the computer memory can stack over flow than using higher order plate finite element or using integration techniques is a solution for this problem. The purpose of this paper is to show the shear locking phenomenon can be avoided by increase low order finite element mesh size of the plates and to study shear locking-free analysis of thick plates using Mindlin's theory by using higher order displacement shape function and to determine the effects of various parameters such as the thickness/span ratio, mesh size on the linear responses of thick plates subjected to uniformly distributed loads. A computer program using finite element method is coded in C++ to analyze the plates clamped or simply supported along all four edges. In the analysis, 4-, 8- and 17-noded quadrilateral finite elements are used. It is concluded that 17-noded finite element converges to exact results much faster than 8-noded finite element, and that it is better to use 17-noded finite element for shear-locking free analysis of plates.

Keywords: thick plate; shear locking; Mindlin's theory; finite element method; 8-noded finite element; 17-noded finite element

1. Introduction

The Reissner-Mindlin plate theory is widely used for thick plates with bending behavior (Reissner 1945). By means of finite element, displacement-based element method is used. Displacement-based finite elements require only C_0 continuity for the three independent kinematic variables: the transverse displacement w and the rotations of the normal vector to the normal vector to the plate middle surface φ_x, φ_y. Despite its simple formulation, whenever the plate thickness is in thin plate limits these displacement-based elements cause a problem known as "shear locking". Moreover, this element can not pass the patch test for the analysis of very thin plates.

In order to eliminate shear locking problem some numerical techniques have been proposed. One of the efficient methods to prevent the appearance of the shear locking phenomenon are reduced and selective integration method (Zienkiewich *et al*. 1971, Hughes *et al*. 1977, Hughes *et al*. 1978). Beside its advantage this method has disadvantage with the poor convergence and the

∗Corresponding author, Associate Professor, E-mail: yaprakozdemir@hotmail.com
[a]Professor, E-mail: yayvaz@yildiz.edu.tr

http://www.techno-press.org/?journal=sem&subpage=8 ISSN: 1225-4568 (Print), 1598-6217 (Online)

presence of some spurious modes. For vanishing these undesirable modes stabilization γ-methods (Flanagan and Belytschko 1981, Belytschko and Stolarski) have been proposed.

A rather heuristic approach to determine whether an element formulation tends to lock or not is proposed by Hughes (2000). The basic idea is to determine the ratio of number of equations to the number of constraints. If this constraint ratio of the discretized system is less than 1.5 then there are more constraints than degrees of freedom and the element will tend to lock if the plate thickness $t_0 \to 0$. Otherwise, if constraint ratio is larger than 1.5 than the Kirchoff-Love constraint will be poorly approximate. This approach can be attributed to Hughes and is used to explain why higher order finite elements are robust with respect to locking (Düster 2001).

Shear locking can be avoided by increasing the mesh size, i.e., using finer mesh, but if the thickness/span ratio is "too small" (Lovadina 1996), convergence may not be achieved even if the finer mesh is used for the first and second order displacement shape functions (4- and 8-noded elements).

The same problem can also be prevented by using higher order displacement shape function (Oloysson 2006), but no references have been found in the literature, which views shear-locking effect in terms of thickness/span ratios, mesh size and boundary condition by comparing with the results of the low order displacement shape function.

The purpose of this paper is to show the shear locking phenomenon can be avoided by increasing low order finite element mesh size of the plates and to study shear locking-free analysis of thick plates referring to Mindlin's theory by using higher order displacement shape function and to determine the effects of various parameters such as the thickness/span ratio, mesh size, the aspect ratio and the boundary conditions on the linear responses of thick plates subjected to uniformly distributed loads. Also the plates are studied with using full, reduced and selective integration techniques. A computer program using finite element method is coded in C++ 6.0 to analyze the plates considered. For the integration of finite element matrix Gauss numerical integration method for two, three and seven sampling points is used. 4-, 8- and 17-noded finite elements are used in the program. 17-noded finite element is obtained by using the fourth order polynomial for the shape function. No references have been found in the literature, which presents results by using 17-noded finite elements. Locking phenomenon is a mesh problem and can be staved off with mesh refinement. If the studier is not preferred going to the solution with increasing mesh size or the computer memory can stack over flow than using higher order plate finite element or using integration techniques is a solution for this problem.

2. Mathematical model

2.1 Mathematical formulation of Mindlin plate theory

In this study, it is assumed that xy plane is the middle surface of the plate and z axis is the normal to the mid-surface, that is $-t/2 \le z \le t/2$, where t is the plate thickness. In the direction of the z axis there is uniformly distributed load $q(x,y)$ applied on the top surface of the plate. In the middle surface of the plate at a point (x,y), displacement components are described as transverse displacement, w, and the rotations φ_x, and φ_y, about the x and y axes, respectively.

2.2 Equilibrium equations

The equilibrium equations in a plate are written as

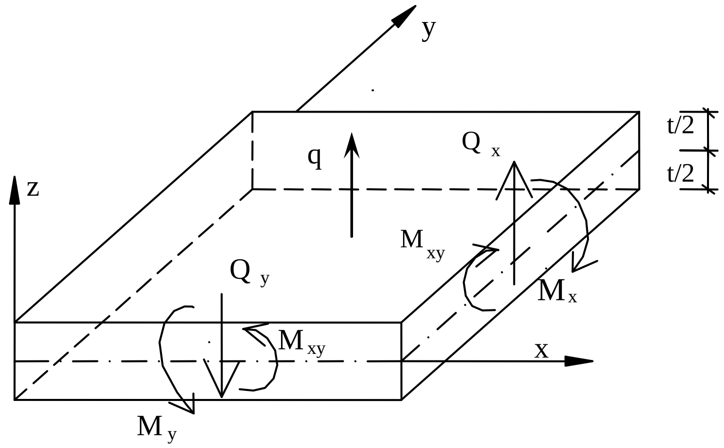

Fig. 1 The positive directions of the external loads and internal forces

$$\frac{\partial M_x}{\partial x} + \frac{\partial M_{xy}}{\partial y} = Q_x \tag{1a}$$

$$\frac{\partial M_{xy}}{\partial x} + \frac{\partial M_y}{\partial y} = Q_y \tag{1b}$$

$$\frac{\partial Q_x}{\partial x} + \frac{\partial Q_y}{\partial y} + q = 0 \tag{1c}$$

where M_x and M_y are the bending moments, M_{xy} represents the twisting moment, Q_x and Q_y are the shear forces. (Fig. 1).

2.3 Strain-displacement relations

The generalized bending strains vector κ and transversal shear strains vector γ are given as follows (Bathe 1996, Ö zdemir 2007)

$$\kappa = \begin{bmatrix} -\frac{\partial \varphi_x}{\partial x} & \frac{\partial \varphi_y}{\partial y} & -\frac{\partial \varphi_x}{\partial y} + \frac{\partial \varphi_y}{\partial x} \end{bmatrix}^T \tag{2a}$$

$$\gamma = \begin{bmatrix} -\varphi_x + \frac{\partial w}{\partial x} & \varphi_y + \frac{\partial w}{\partial y} \end{bmatrix}^T \tag{2b}$$

where T stands for matrix transpose.

2.4 Boundary conditions

In this study, since the plate considered are clamped or simply supported along all four edges,

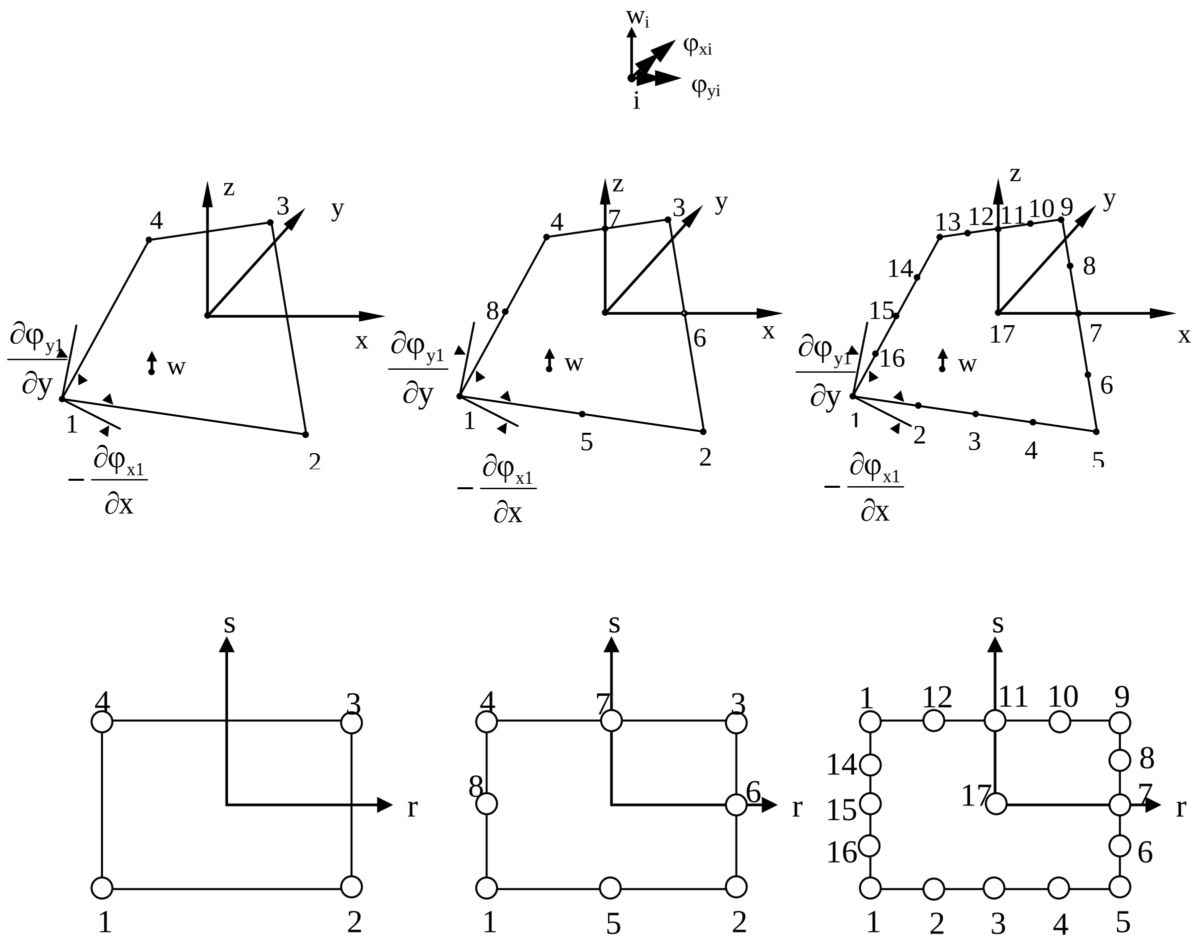

Fig. 2 4-, 8-, and 17-noded finite element models used in this study

the following boundary conditions are used (see Fig. 2).

For clamped plates (see Fig. 2);

Along $x = -a/2$ and $x = a/2$; $\varphi_x = 0$ and $w_0 = 0$.

Along $y = -b/2$ and $y = b/2$; $\varphi_y = 0$ and $w_0 = 0$.

For simply supported plates (see Fig. 2);

Along $x = -a/2$ and $x = a/2$; $M_x = 0$ and $w_0 = 0$.

Along $y = -b/2$ and $y = b/2$; $M_y = 0$ and $w_0 = 0$.

3. Finite element formulation of the problem

In this study, 4-, 8-, and 17-noded finite elements are presented, in which the transverse displacement and rotations are interpolated with usage of independent shape functions.

Considering the plate with *q* which is equal to the transverse loading per unit of the midsurface area *A*, the expression for the principle of virtual work is, given as

$$\Pi = \frac{1}{2}\int_A \int_{-t/2}^{t/2} \kappa^T \bar{E}_\kappa \kappa d_A + \frac{k}{2}\int_A \int_{-t/2}^{t/2} \gamma^T \bar{E}_\gamma \gamma d_A - \int_A \int_{-t/2}^{t/2} q w d_A \tag{3}$$

where *k* is a constant to account for the actual nonuniformity of the shearing stresses, $\bar{E}_\kappa \kappa$ and $\bar{E}_\gamma \gamma$ are the internal bending moments and shear forces, respectively. $\bar{E}_\kappa$ and $\bar{E}_\gamma$ are given as follows (Reissner 1950)

$$\bar{E}_\kappa = E_\kappa \frac{t^3}{12}; \qquad \bar{E}_\gamma = kE_\gamma t. \tag{4}$$

where E_κ and E_γ are the elasticity matrix and these matrices are given as

$$E_\kappa = \frac{E}{(1-\nu^2)}\begin{bmatrix} 1 & \nu & 0 \\ \nu & 1 & 0 \\ 0 & 0 & \frac{1-\nu}{2} \end{bmatrix} \qquad E_\gamma = \frac{E}{2(1+\nu)}\begin{bmatrix} 1 & 0 \\ 0 & 1 \end{bmatrix}. \tag{5}$$

where *E* is the Modulus of elasticity and *v* is the Poisson’s ratio.

If internal stresses are written in a matrix form; the following equation can be obtained

$$\begin{Bmatrix} \sigma_x \\ \sigma_y \\ \tau_{xy} \\ \tau_{xz} \\ \tau_{yz} \end{Bmatrix} = \begin{bmatrix} \frac{E}{(1-\nu^2)} & \frac{\nu E}{(1-\nu^2)} & 0 & 0 & 0 \\ \frac{\nu E}{(1-\nu^2)} & \frac{E}{(1-\nu^2)} & 0 & 0 & 0 \\ 0 & 0 & \frac{E}{2(1+\nu)} & 0 & 0 \\ 0 & 0 & 0 & \frac{E}{2(1+\nu)} & 0 \\ 0 & 0 & 0 & 0 & \frac{E}{2(1+\nu)} \end{bmatrix} \begin{Bmatrix} \varepsilon_x \\ \varepsilon_y \\ \gamma_{xy} \\ \gamma_{xz} \\ \gamma_{yz} \end{Bmatrix}. \tag{6}$$

Generalized stresses are written in a matrix form and calculated as

$$\{M\} = [\bar{E}]\{\varepsilon\}. \tag{7}$$

The nodal displacements for these elements can be written as follows (Mindlin 1951)

$$u=\{u, v, w\}=\{-z\varphi_x, z\varphi_y, w\} \tag{8}$$

$$u=-z\varphi_x=-z\sum_{1}^{8\,\mathrm{or}\,17} h_i \varphi_{xi}, \quad v=z\varphi_y=z\sum_{1}^{8\,\mathrm{or}\,17} h_i \varphi_{yi}, \quad w=\sum_{1}^{8\,\mathrm{or}\,17} h_i w_i \quad \begin{matrix} i=1,2,3,4 \text{ for 4-noded element} \\ i=1,\ldots,8 \text{ for 8-noded element} \\ i=1,\ldots,17 \text{ for 17-noded element} \end{matrix} \tag{9}$$

Where *w* is the displacement and φ_x and φ_y are the rotations in the *x* and *y* directions, respectively. Nodal force corresponding to the displacements in Eq. (8) are

$$q_i=\{q_{i1}, q_{i2}, q_{i3}\}=\{M_{xi}, M_{yi}, q_{zi}\} \quad \begin{array}{l} \text{i = 1,2,3,4 for 4 - noded element} \\ \text{i=1,...,8 for 8-noded element} \\ \text{i =1,...,17 for 17 - noded element} \end{array} \tag{10}$$

The symbols q_{zi} denotes a force in the *z* direction, but M_{xi} and M_{yi} are the moments in the *x* and *y* directions, respectively. Note that these fictitious moments at the nodes are not the same as the distributed moments in the vector *M* of generalized stresses (Weaver and Jahnston 1984)

The displacement functions for 4-noded, 8-noded (Weaver and Janston 1984, Bathe 1996, Cook *et al*. 1989), and 17-noded elements are given by Eq. (11a), Eq. (11b), and Eq. (11c), respectively

$$w=c_1+c_2r+c_3s+c_4rs \tag{11a}$$

$$w=c_1+c_2r+c_3s+c_4r^2+c_5rs+c_6s^2+c_7r^2s+c_8rs^2. \tag{11b}$$

$$\begin{aligned} w &= c_1+c_2r+c_3s+c_4r^2+c_5rs+c_6s^2+c_7r^2s+c_8rs^2+c_9r^3+c_{10}r^3s+c_{11}rs^3 \\ &\quad +c_{12}s^3+c_{13}r^2s^2+c_{14}r^4+c_{15}r^4s+c_{16}rs^4+c_{17}s^4. \end{aligned} \tag{11c}$$

From Eq. (11), it is possible to derive the displacement shape function for 4-noded element with Eq. (12a), 8-noded element with Eq. (12b) and 17-noded element with Eq. (12c)

$$h_{4i}=[h_1,h_2,h_3,h_4] \tag{12a}$$

$$h_{8i}=[h_1,h_2,h_3,h_4,h_5,h_6,h_7,h_8] \tag{12b}$$

$$h_{17i}=[h_1,h_2,h_3,h_4,h_5,h_6,h_7,h_8,h_9,h_{10},h_{11},h_{12},h_{13},h_{14},h_{15},h_{16},h_{17}] \tag{12c}$$

Where

$$\begin{aligned} h_1 &= (0.25)*(1+r)*(1+s), \quad h_2=(0.25)*(1-r)*(1+s), \\ h_3 &= (0.25)*(1-r)*(1-s), \quad h_4=(0.25)*(1+r)*(1-s), \end{aligned} \tag{13a}$$

are given with Eq. (13a)

$$\begin{aligned} h_1 &= (0.25)*(1-r)*(1-s)*(-r-s-1), \quad h_2=(0.5)*(1-r*r)*(1-s), \\ h_3 &= (0.25)*(1+r)*(1-s)*(r-s-1), \quad h_4=(0.5)*(1+r)*(1-s*s), \\ h_5 &= (0.25)*(1+r)*(1+s)*(r+s-1), \quad h_6=(0.5)*(1-r*r)*(1+s), \\ h_7 &= (0.25)*(1-r)*(1+s)*(-r+s-1), \quad h_8=(0.5)*(1-r)*(1-s*s) \end{aligned} \tag{13b}$$

are given with Eq. (13b)

$$\begin{aligned} h_1 &= \left(\frac{1}{3}\right)r+\left(\frac{1}{3}\right)s-\left(\frac{5}{12}\right)r*s-\left(\frac{1}{3}\right)r^2+\left(\frac{1}{12}\right)r^2*s+\left(\frac{1}{12}\right)r*s^2-\left(\frac{1}{3}\right)s^2-\left(\frac{1}{3}\right)r^3+\left(\frac{1}{3}\right)r^3*s \\ &\quad +\left(\frac{1}{3}\right)r*s^3-\left(\frac{1}{3}\right)s^3+\left(\frac{1}{4}\right)r^2*s^2+\left(\frac{1}{3}\right)r^4-\left(\frac{1}{3}\right)r^4*s-\left(\frac{1}{3}\right)r*s^4+\left(\frac{1}{3}\right)s^4 \\ h_2 &= -\left(\frac{2}{3}\right)r+\left(\frac{2}{3}\right)r*s+\left(\frac{4}{3}\right)r^2-\left(\frac{4}{3}\right)r^2*s+\left(\frac{2}{3}\right)r^3-\left(\frac{2}{3}\right)r^3*s-\left(\frac{4}{3}\right)r^4+\left(\frac{4}{3}\right)r^4*s \end{aligned}$$

$$h_3 = -\left(\frac{1}{2}\right)s - (2)r^2 + \left(\frac{5}{2}\right)r^2 * s + \left(\frac{1}{2}\right)s^2 - \left(\frac{1}{2}\right)r^2 * s^2 + (2)r^4 - (2)r^4 * s$$

$$h_4 = \left(\frac{2}{3}\right)r - \left(\frac{2}{3}\right)r * s + \left(\frac{4}{3}\right)r^2 - \left(\frac{4}{3}\right)r^2 * s - \left(\frac{2}{3}\right)r^3 + \left(\frac{2}{3}\right)r^3 * s - \left(\frac{4}{3}\right)r^4 + \left(\frac{4}{3}\right)r^4 * s$$

$$h_5 = -\left(\frac{1}{3}\right)r + \left(\frac{1}{3}\right)s + \left(\frac{5}{12}\right)r * s - \left(\frac{1}{3}\right)r^2 + \left(\frac{1}{12}\right)r^2 * s - \left(\frac{1}{12}\right)r * s^2 - \left(\frac{1}{3}\right)s^2 + \left(\frac{1}{3}\right)r^3 - \left(\frac{1}{3}\right)r^3 * s$$
$$- \left(\frac{1}{3}\right)r * s^3 - \left(\frac{1}{3}\right)s^3 + \left(\frac{1}{4}\right)r^2 * s^2 + \left(\frac{1}{3}\right)r^4 - \left(\frac{1}{3}\right)r^4 * s + \left(\frac{1}{3}\right)r * s^4 + \left(\frac{1}{3}\right)s^4$$

$$h_6 = -\left(\frac{2}{3}\right)s + \left(\frac{2}{3}\right)r * s + \left(\frac{4}{3}\right)r * s^2 + \left(\frac{4}{3}\right)s^2 + \left(\frac{2}{3}\right)r * s^3 + \left(\frac{2}{3}\right)s^3 - \left(\frac{4}{3}\right)r * s^4 - \left(\frac{4}{3}\right)s^4$$

$$h_7 = \left(\frac{1}{2}\right)r + \left(\frac{1}{2}\right)r^2 - \left(\frac{5}{2}\right)r * s^2 - (2)s^2 - \left(\frac{1}{2}\right)r^2 * s^2 + (2)r * s^4 + (2)s^4$$

$$h_8 = \left(\frac{2}{3}\right)s + \left(\frac{2}{3}\right)r * s + \left(\frac{4}{3}\right)r * s^2 + \left(\frac{4}{3}\right)s^2 - \left(\frac{2}{3}\right)r * s^3 - \left(\frac{2}{3}\right)s^3 - \left(\frac{4}{3}\right)r * s^4 - \left(\frac{4}{3}\right)s^4$$

$$h_9 = -\left(\frac{1}{3}\right)r - \left(\frac{1}{3}\right)s - \left(\frac{5}{12}\right)r * s - \left(\frac{1}{3}\right)r^2 - \left(\frac{1}{12}\right)r^2 * s - \left(\frac{1}{12}\right)r * s^2 - \left(\frac{1}{3}\right)s^2 + \left(\frac{1}{3}\right)r^3 + \left(\frac{1}{3}\right)r^3 * s$$
$$+ \left(\frac{1}{3}\right)r * s^3 + \left(\frac{1}{3}\right)s^3 + \left(\frac{1}{4}\right)r^2 * s^2 + \left(\frac{1}{3}\right)r^4 + \left(\frac{1}{3}\right)r^4 * s + \left(\frac{1}{3}\right)r * s^4 + \left(\frac{1}{3}\right)s^4$$

$$h_{10} = \left(\frac{2}{3}\right)r + \left(\frac{2}{3}\right)r * s + \left(\frac{4}{3}\right)r^2 + \left(\frac{4}{3}\right)r^2 * s - \left(\frac{2}{3}\right)r^3 - \left(\frac{2}{3}\right)r^3 * s - \left(\frac{4}{3}\right)r^4 - \left(\frac{4}{3}\right)r^4 * s$$

$$h_{11} = \left(\frac{1}{2}\right)s - (2)r^2 - \left(\frac{5}{2}\right)r^2 * s + \left(\frac{1}{2}\right)s^2 - \left(\frac{1}{2}\right)r^2 * s^2 + (2)r^4 + (2)r^4 * s$$

$$h_{12} = -\left(\frac{2}{3}\right)r - \left(\frac{2}{3}\right)r * s + \left(\frac{4}{3}\right)r^2 + \left(\frac{4}{3}\right)r^2 * s + \left(\frac{2}{3}\right)r^3 + \left(\frac{2}{3}\right)r^3 * s - \left(\frac{4}{3}\right)r^4 - \left(\frac{4}{3}\right)r^4 *$$

$$h_{13} = \left(\frac{1}{3}\right)r - \left(\frac{1}{3}\right)s + \left(\frac{5}{12}\right)r * s - \left(\frac{1}{3}\right)r^2 - \left(\frac{1}{12}\right)r^2 * s + \left(\frac{1}{12}\right)r * s^2 - \left(\frac{1}{3}\right)s^2 - \left(\frac{1}{3}\right)r^3 - \left(\frac{1}{3}\right)r^3 * s$$
$$- \left(\frac{1}{3}\right)r * s^3 + \left(\frac{1}{3}\right)s^3 + \left(\frac{1}{4}\right)r^2 * s^2 + \left(\frac{1}{3}\right)r^4 + \left(\frac{1}{3}\right)r^4 * s - \left(\frac{1}{3}\right)r * s^4 + \left(\frac{1}{3}\right)s^4$$

$$h_{14} = \left(\frac{2}{3}\right)s - \left(\frac{2}{3}\right)r * s - \left(\frac{4}{3}\right)r * s^2 + \left(\frac{4}{3}\right)s^2 + \left(\frac{2}{3}\right)r * s^3 - \left(\frac{2}{3}\right)s^3 + \left(\frac{4}{3}\right)r * s^4 - \left(\frac{4}{3}\right)s^4$$

$$h_{15} = -\left(\frac{1}{2}\right)r + \left(\frac{1}{2}\right)r^2 + \left(\frac{5}{2}\right)r * s^2 - (2)s^2 - \left(\frac{1}{2}\right)r^2 * s^2 - (2)r * s^4 + (2)s^4$$

$$h_{16} = -\left(\frac{2}{3}\right)s + \left(\frac{2}{3}\right)r * s - \left(\frac{4}{3}\right)r * s^2 + \left(\frac{4}{3}\right)s^2 - \left(\frac{2}{3}\right)r * s^3 + \left(\frac{2}{3}\right)s^3 + \left(\frac{4}{3}\right)r * s^4 - \left(\frac{4}{3}\right)s^4$$

$$h_{17} = 1 - r^2 - s^2 + r^2 * s^2 \tag{13c}$$

are given with Eq. (13c), (Özdemir 2007, Özdemir *et al*. 2007)

The subscripts in the vector of h stand for the node number of 4-, 8- or 17-noded quadrilateral finite element.

The strain vector in Eq. (7) for these elements can be written as follows

$$\{\varepsilon\} = \begin{bmatrix} \varepsilon_x \\ \varepsilon_y \\ \gamma_{xy} \\ \gamma_{xz} \\ \gamma_{yz} \end{bmatrix} = \begin{bmatrix} u,_x \\ v,_y \\ u,_y + v,_x \\ u,_z + w,_x \\ v,_z + w,_y \end{bmatrix}. \tag{14}$$

Before formulating element stiffness matrix, strain-displacement matrix B is partitioned as follows

$$B = \begin{bmatrix} B_k \\ B_\gamma \end{bmatrix} = \begin{bmatrix} z\overline{B}_k \\ B_\gamma \end{bmatrix}. \tag{15}$$

Where B_k is the bending strain matrix and B_γ is the shear strain matrix. These matrices are given by the following equations.

$$B_{k_i} = \begin{bmatrix} 0 & 0 & -\dfrac{\partial h_i}{\partial x} \\ 0 & \dfrac{\partial h_i}{\partial y} & 0 \\ 0 & \dfrac{\partial h_i}{\partial x} & -\dfrac{\partial h_i}{\partial y} \end{bmatrix}_{\substack{3x12\ for\ 4-noded\ finite\ element \\ 3x24\ for\ 8-noded\ finite\ element \\ 3x51\ for\ 17-noded\ finite\ element}} \qquad \begin{array}{l} i = 1,2,3,4 \text{ for 4 - noded element} \\ i = 1,\dots,8 \text{ for 8-noded element} \\ i = 1,\dots,17 \text{ for 17 - noded element} \end{array}$$

$$B_{\gamma_i} = \begin{bmatrix} \dfrac{\partial h_i}{\partial x} & 0 & -h_i \\ \dfrac{\partial h_i}{\partial y} & h_i & 0 \end{bmatrix}_{\substack{2x12\ for\ 4-noded\ finite\ element \\ 2x24\ for\ 8-noded\ finite\ element \\ 2x51\ for\ 17-noded\ finite\ element}} \qquad \begin{array}{l} i = 1,2,3,4 \text{ for 4 - noded element} \\ i = 1,\dots,8 \text{ for 8-noded element} \\ i = 1,\dots,17 \text{ for 17 - noded element} \end{array} \tag{16}$$

Where B_k is the size of 3×12, 3×24, 3×51 for 4-, 8-, and 17-noded quadrilateral elements, respectively and B_γ is the size of 2×12, 2×24, 2×51 for 4-, 8-, and 17-noded rectangular elements, respectively. The matrix B for each element can be written as follows

$$[B] = \begin{bmatrix} 0 & 0 & -\dfrac{\partial h_i}{\partial x} & \dots \\ 0 & \dfrac{\partial h_i}{\partial y} & 0 & \dots \\ 0 & \dfrac{\partial h_i}{\partial x} & -\dfrac{\partial h_i}{\partial y} & \dots \\ \dfrac{\partial h_i}{\partial x} & 0 & -h_i & \dots \\ \dfrac{\partial h_i}{\partial y} & h_i & 0 & \dots \end{bmatrix}_{\substack{5x12\ for\ 4-noded\ finite\ element \\ 5x24\ for\ 8-noded\ finite\ element \\ 5x51\ for\ 17-noded\ finite\ element}} \qquad \begin{array}{l} i = 1,2,3,4 \text{ for 4 - noded element} \\ i = 1,\dots,8 \text{ for 8-noded element} \\ i = 1,\dots,17 \text{ for 17 - noded element} \end{array} \tag{17}$$

Then the stiffness matrices for these elements are written as

$$K = \int_V B^T E B dV = \int_V \left[z\overline{B}_k^T \quad B_\gamma^T \right] \begin{bmatrix} E_k & 0 \\ 0 & E_\gamma \end{bmatrix} \begin{bmatrix} z\overline{B}_k^T \\ B_\gamma^T \end{bmatrix} dV$$
$$K = \int_V \left(z^2 \overline{B}_k^T E_k \overline{B}_k \right) + \left(\overline{B}_\gamma^T E_\gamma \overline{B}_\gamma \right) dV. \tag{18}$$

Integration of Eq. (17) through the thickness yields

$$K = \int_A \left(\overline{B}_k^T \overline{E}_k \overline{B}_k + \overline{B}_\gamma^T \overline{E}_\gamma \overline{B}_\gamma \right) dA. \tag{19}$$

Thus, Eq. (17) can be rewritten in the following form.

$$K = \int_A \overline{B}^T \overline{E}\overline{B} dA = \int_{-1}^{1} \int_{-1}^{1} \overline{B}^T \overline{E}\overline{B} |J| dr ds \tag{20}$$

which must be evaluated numerically (Bathe 1996).

The matrices which show the displacements and rotations in the plate for 4-, 8- and 17-noded elements, are given by the following three equations.

$$\hat{u}^T = \lfloor \varphi_{x_1} \quad \varphi_{y_1} \quad w_1; \dots \quad ; \varphi_{x_4} \quad \varphi_{y_4} \quad w_4 \rfloor \tag{20a}$$

$$\hat{u}^T = \lfloor \varphi_{x_1} \quad \varphi_{y_1} \quad w_1; \dots \quad ; \varphi_{x_8} \quad \varphi_{y_8} \quad w_8 \rfloor \tag{20b}$$

$$\hat{u}^T = \lfloor \varphi_{x_1} \quad \varphi_{y_1} \quad w_1; \dots \quad ; \varphi_{x_{17}} \quad \varphi_{y_{17}} \quad w_{17} \rfloor \tag{20c}$$

The values of these matrixes can be calculated with the Gauss Integration method. 2 gauss points for 4-noded finite element, 3 gauss points for 8-noded finite element and 5 gauss points for 17-noded finite element are sufficient. Then the strains are calculated by the following equation;

$$\{\varepsilon\} = [B]\{u\} \tag{21}$$

After finding the strains, the stresses of the plate can be calculated by Eq. (6).

4. Numerical examples

4.1 Data

A number of examples are considered to examine the performance of 4- noded (MT4), 8-noded (MT8), and 17-noded (MT17) elements on both displacements and bending moments with a coded computer programme.

A square plate which is subjected to a uniformly distributed load is modeled with two different boundary conditions, i.e., either simply supported or clamped along all four edges, to evaluate

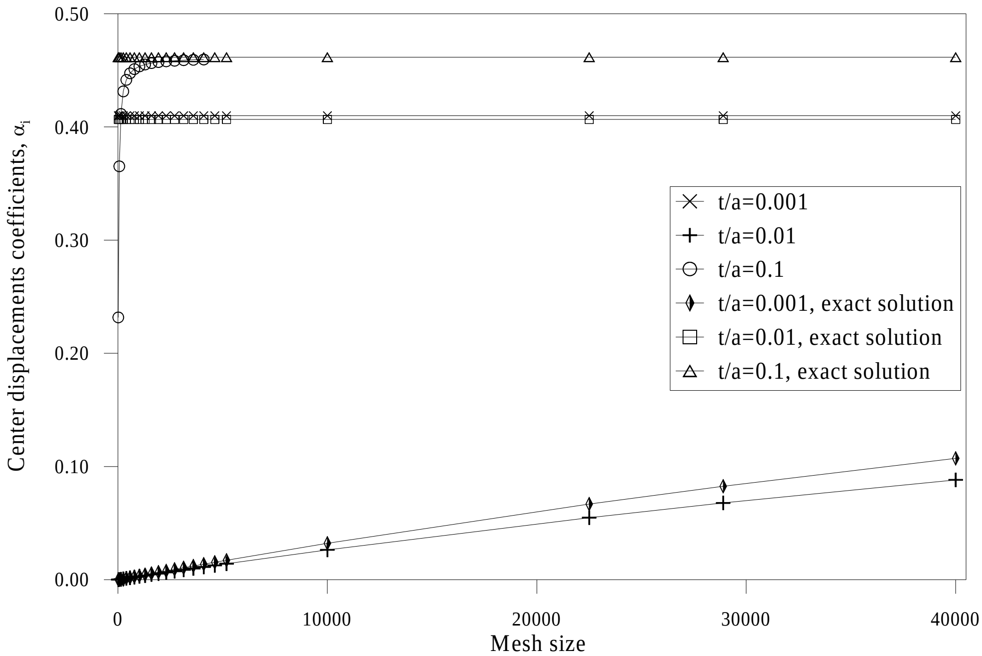

Fig. 3 Center displacement coefficients, αi, of the simply supported square plates modeling with MT4 for different mesh sizes and *t/a* ratios

the acceptability of the solutions obtained with MT4, MT8, and MT17 elements. The geometric and material properties are used E=2.7*10^6 kN/m^2, ν= 0.3, a=b=3 m, q_z=20 kN/m^2, and k=5/6, where q_z is the uniformly distributed load, and a is the smaller span length of the plate. In the analysis, the full plate is used.

4.2 Results

In this study, the maximum displacement and bending moment coefficients for different thickness/span ratios and the maximum displacements and bending moments for different aspect ratios are presented. This simplification to maximum responses is supported by the fact that maximum values of these quantities are the most important ones for design.

In order to understand better the linear response of thick plates subjected to uniformly distributed loads, the results are presented in tables and graphs. The maximum displacement and bending moment coefficients for different thickness/span ratios and mesh sizes, and the maximum bending moment coefficient for different thickness/span ratios are given in Tables 1, 2 and 3, respectively, for clamped plates. The maximum displacement and bending moment coefficient for different mesh sizes and thickness/span ratios are given in Tables 4, 5 and 6 for simply supported plates. These values are also presented in graphical form in Figs. 3, 4, and 5, respectively.

As seen from Tables 1, 2 center displacement coefficients, α_i, of the clamped plates obtained in this study are very close to the exact solution for MT8 and MT17 elements. Besides shear locking problem can be seen clearly for MT4 element for 0.001, 0.01, and 0.1 *t/a* ratios and MT8 elements for 0.001, 0.01 *t/a* ratios different mesh sizes.

Table 1 Center displacements coefficients, αi, $(=\omega/(qa4/100D))$ of the clamped square plate for different mesh sizes and *t/a* ratios

t/a	α_i						
	This study (MT8,24 dof.)			This study (MT17,51 dof.)			Exact, (Soh *et al*. 2001) thick
	Mesh size			Mesh size			
	4×4	8×8	16×16	4×4	8×8	16×16	
0.001	0.0005	0.0499	0.1227	0.1011	0.1252	0.1265	0.1265
0.01	0.0359	0.1189	0.1256	0.1230	0.1268	0.1268	0.1265
0.10	0.1420	0.1499	0.1504	0.1503	0.1505	0.1505	0.1499
0.15	0.1745	0.1785	0.1787	0.1786	0.1788	0.1788	0.1798
0.20	0.2146	0.2170	0.2172	0.2171	0.2172	0.2172	0.2167
0.25	0.2639	0.2657	0.2658	0.2657	0.2658	0.2658	-
0.30	0.3230	0.3245	0.3246	0.3245	0.3246	0.3246	0.3227
0.35	0.3922	0.3936	0.3937	0.3935	0.3937	0.3937	0.3951

Table 2 Center displacements coefficients, α_i, $(=\omega_/(qa^4/100D))$ of the clamped square plate for different *t/a* ratios

t/a	α_i										
	(Ç elik 1996)	(Yuqiu and Fei 1992)	(Ozkul and Ture 2004) (16×16 meshes)	(Yuan and Miller 1988)	(Yuan and Miller 1989)	(Owen and Zienkiew icz 1982)	(Soh *et al*. 2001) (16×16 meshes)	This study			Exact, (Soh *et al*. 2001) thick
								MT4 (20×20 meshes)	MT8 (16×16 meshes)	MT17 (8×8 meshes)	
0.001	0.1265	0.1293	0.1256	0.1234	0.1255	0.1220	0.1279	0.0002	0.1227	0.1252	0.1265
0.01	0.1284	0.1293	0.1267	0.1236	0.1267	0.1230	0.1281	0.0195	0.1256	0.1268	0.1265
0.10	0.1584	0.1521	0.1506	0.1482	0.1513	0.1460	0.1514	0.1433	0.1504	0.1505	0.1499
0.15	0.1859	0.1801	0.1787	0.1776	0.1807	-	-	0.1752	0.1787	0.1788	0.1798
0.20	0.2236	0.2181	0.2172	0.2171	0.2203	0.2110	0.2183	0.2151	0.2172	0.2172	0.2167
0.25	0.2716	0.2658	-	-	0.2700	-	-	0.2644	0.2658	0.2658	-
0.30	0.3299	0.3229	-	-	-	-	0.3259	0.3236	0.3246	0.3246	0.3227
0.35	0.3987	0.3896	-	-	-	-	0.3952	0.3930	0.3937	0.3937	0.3951

As seen from Table 3, center moment coefficients, β_i, of the clamped plates obtained in this study with for MT8 and MT17 elements are very close to the exact solution of thin plate. Besides shear locking problem can be seen clearly for MT4 element for different for 0.001 and 0.01 *t/a* ratios.

As seen from Tables 4, 5 and and Figs. 3, 4, and 5, center displacement coefficients, α_i, of the simply supported plates obtained in this study are very close to the exact solution for MT8 and MT17 elements. As also seen from Tables 4, 5 and Fig. 5, the results obtained by using 17-noded finite element almost coincide with the exact result for 0.1 *t/a* ratio. The solutions obtained in this study coincide with the exact solution for 0.1 *t/a* ratio if 8×8 mesh sizes (64 elements) are used for MT17 element and 32×32 mesh sizes (1024 elements) are used for MT8 element.

As seen from Tables 4, 6, center moment coefficients, β_i, of the simply supported plates obtained in this study are very close to the exact solution for MT8 and MT17 elements. As also

Table 3 Maximum bending moment coefficients, βi, (=M/(qa2/10)) at the center of the clamped square plates

t/a	β_i							
	(Çelik 1996)	(Ozkul and Ture 2004) (16×16 meshes)	(Owen and Zienkiewicz)	(Soh *et al*. 2001) (16×16 meshes)	This study			Exact (Timoshenko and Krieger 1959) thin
					MT4 (20×20 meshes)	MT8 (12×12 meshes)	MT17 (8×8 meshes)	
0.001	0.2300	0.2294	0.2270	0.2069	0.0005	0.2249	0.2209	0.231
0.01	0.2340	0.2301	0.2270	0.2069	0.0375	0.2280	0.2290	0.231
0.10	0.2530	0.2331	0.236	0.2070	0.2200	0.2322	0.2320	0.231
0.15	0.2540	0.2352	-	-	0.2280	0.2344	0.2340	0.231
0.20	0.2550	0.2370	0.250	0.2071	0.2318	0.2361	0.2357	0.231
0.25	0.2550	-	-	-	0.2340	0.2374	0.2370	0.231
0.30	0.2550	-	-	-	0.2355	0.2384	0.2380	0.231
0.35	0.2550	-	-	-	0.2365	0.2391	0.2386	0.231

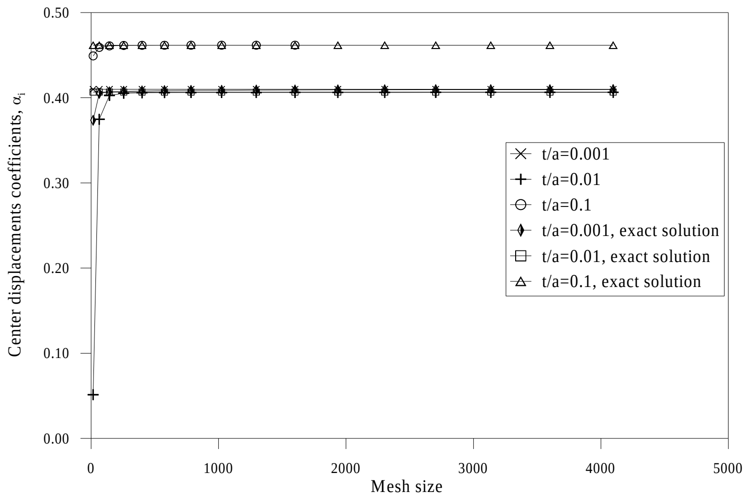

Fig. 4 Center displacement coefficients, αi, of the simply supported square plates modeling with MT8 for different mesh sizes and *t/a* ratios

seen from Tables 4, 6, the results obtained by using 17-noded finite element almost coincide with the exact result for 0.1 *t/a* ratio. The solutions obtained in this study coincide with the exact solution for 0.1 *t/a* ratio if 8×8 mesh sizes (64 elements) are used for MT17 element and 32×32 mesh sizes (1024 elements) are used for MT8 element.

As seen from Tables 1, 2, 3, 4, 5 and 6, and Figs. 3, 4, 5, and 6, the results obtained in this study by using MT17 element converges rapidly to the exact results than the results given in the literature. By using this element, the mesh size required to produce the desired accuracy can be approximately reduced to the half of those of the given in the other literature, (Çelik 1996, Yuqiu and Fei 1992, Ozkul and Ture 2004, Yuan and Miller 1989, Owen and Zienkiewicz, 1982, Soh *et al*. 2001, Ibrahimbegovic 1993, Zienkiewicz *et al*. 1993, Panc 1975, Belounar and Guenfoud 2005, Cen *et al*. 2006).

Table 4 Center displacements coefficients, αi, (=$w/(qa4/100D)$) and bending moment coefficients, βi, (=$M/(qa2/10)$) of the simply supported square plates for different mesh sizes

(a) Thickness/span ratio t/a=0.001

Mesh	α_i						β_i					
	(Soh *et al.* 2001)	(Ibrahimbegovic 1993)	(Zienkiewicz *et al.* 1993)	MT4	MT8	MT17	(Soh *et al.* 2001)	(Ibrahimbegovic 1993)	(Zienkiewicz *et al.* 1993)	MT4	MT8	MT17
4×4	0.4045	0.4045	0.4593	0.0001	0.0513	0.4004	0.5009	0.5005	0.5649	0.0001	0.0616	0.4721
8×8	0.4060	0.4060	0.4292	0.0002	0.3747	0.4062	0.4839	0.4839	0.5010	0.0002	0.4454	0.4776
16×16	0.4062	0.4062	0.4164	0.0007	0.4053	0.4063	0.4801	0.4801	0.4876	0.0009	0.4775	0.4781
32×32	0.4062	0.4062	0.4110	0.0029	0.4062	0.4063	0.4792	0.4792	0.4830	0.0286	0.4785	0.4790
Exact, (Soh *et al.* 2001) thick	0.4066						0.4792					
Exact (Panc 1975) thin	0.4062						0.4789					

(b) Thickness/span ratio t/a=0.01

Mesh	α_i						β_i					
	(Soh *et al.* 2001)	(Ibrahimbegovic 1993)	(Zienkiewicz *et al.* 1993)	MT4	MT8	MT17	(Soh *et al.* 2001)	(Ibrahimbegovic 1993)	(Zienkiewicz *et al.* 1993)	MT4	MT8	MT17
4×4	0.4047	0.4461	0.4596	0.0045	0.3735	0.4072	0.5007	0.5659	0.5649	0.0048	0.4405	0.4763
8×8	0.4062	0.4227	0.4297	0.0173	0.4051	0.4083	0.4842	0.5081	0.5012	0.0205	0.4766	0.4805
16×16	0.4064	0.4140	0.4172	0.0613	0.4075	0.4093	0.4804	0.4892	0.4882	0.0741	0.4797	0.4811
32×32	0.4067	0.4106	0.4124	0.1690	0.4087	0.4098	0.4797	0.4835	0.4841	0.2039	0.4808	0.4820
Exact, (Soh *et al.* 2001) thick	0.4099						0.4820					
Exact (Panc 1975) thin	0.4064						0.4789					

(c) Thickness/span ratio t/a=0.1

Mesh	α_i						β_i					
	(Soh *et al.* 2001)	(Ibrahimbegovic 1993)	(Zienkiewicz *et al.* 1993)	MT4	MT8	MT17	(Soh *et al.* 2001)	(Ibrahimbegovic 1993)	(Zienkiewicz *et al.* 1993)	MT4	MT8	MT17
4×4	0.4280	0.4774	0.4957	0.3587	0.4491	0.4611	0.5206	0.5808	0.5694	0.5808	0.5011	0.5091
8×8	0.4419	0.4612	0.4727	0.4311	0.4591	0.4617	0.5087	0.5238	0.5169	0.5238	0.5076	0.5095
16×16	0.4544	0.4600	0.4644	0.4525	0.4614	0.4617	0.5081	0.5117	0.5112	0.5117	0.5094	0.5096
32×32	0.4596	0.4610	0.4624	-	0.4617	0.4617	0.5091	0.5099	0.5100	0.5099	0.5096	0.5096
Exact, (Soh *et al.* 2001) thick	0.4617						0.5096					
Exact (Panc 1975) thin	0.4273						0.4789					

Table 5 Center displacements coefficients, αi, ($=\omega/(qa4/100D)$) of the simply supported square plate for different t/a ratios

t/a	α_i								
	(Yuqiu and Fei 1992)	(Ozkul and Ture 2004) (16×16 meshes)	(Yuan and Miller 1988)	(Owen and Zienkiewicz 1982)	(Soh *et al.* 2001) (16×16 meshes)	This study MT4 (20×20 meshes)	This study MT8 (16×16 meshes)	This study MT17 (8×8 meshes)	Exact, (Soh *et al.* 2001) Thick/thin
0.001	0.4043	0.4060	0.4054	0.4070	0.4062	0.0014	0.4053	0.4062	0.4066/0.4062
0.01	0.4045	0.4064	0.4067	0.4070	0.4064	0.1068	0.4075	0.4083	0.4099/0.4064
0.10	0.4242	0.4278	0.4596	0.4230	0.4544	0.4879	0.4614	0.4617	0.4617/0.4273
0.15	0.4502	0.4536	0.5018	-	-	0.5117	0.5036	0.5037	-/-
0.20	0.4869	0.4904	0.5511	0.4800	-	0.5281	0.5544	0.5545	-/0.4906
0.25	-	-	-	-	-	0.5410	0.6140	0.6140	-/-
0.30	-	-	-	-	-	0.5514	0.6823	0.6823	-/0.5956
0.35	-	-	-	-	-	0.5600	0.7595	0.7595	-/0.6641

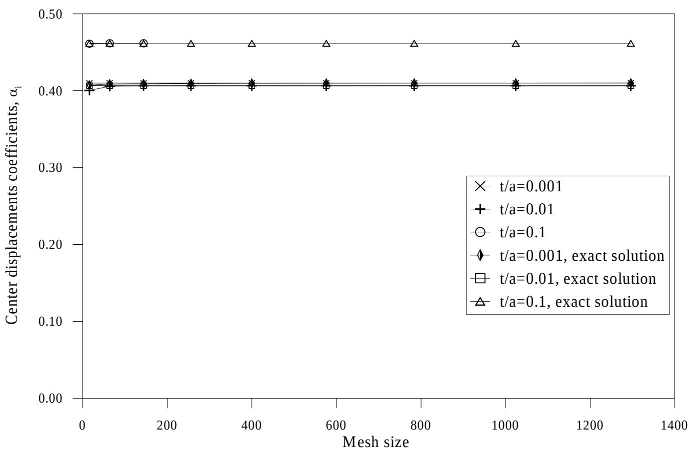

Fig. 5 Center displacement coefficients, αi, of the simply supported square plates modeling with MT17 for different mesh sizes and *t/a* ratios

Table 6 Center bending moment coefficients, βi, ($=M/(qa2/10)$) of the simply supported square plate for different t/a ratios

t/a	β_i							
	(Ozkul and Ture 2004) (16×16 meshes)	(Yuan and Miller 1988)	(Owen and Zienkiewicz 1982)	(Soh *et al.* 2001) (16×16 meshes)	This study MT4 (20×20 meshes)	This study MT8 (16×16 meshes)	This study MT17 (8×8 meshes)	Exact (Soh *et al.* 2001) Thick/thin
0.001	0.4795	0.4779	0.4820	0.4801	0.0011	0.4750	0.4776	0.4792/0.4789
0.01	0.4795	0.4788	0.4820	0.4804	0.0883	0.4797	0.4805	0.4820/0.4789
0.10	0.4795	0.5079	0.4840	0.5081	0.4416	0.5094	0.5095	0.5096/0.4789
0.15	0.4795	0.5223	-	-	0.4928	0.5236	0.5236	-/-
0.20	0.4795	0.5350	-	-	0.5473	0.5363	0.5362	-/-
0.25	-	-	-	-	0.6088	0.5472	0.5471	-/-
0.30	-	-	-	-	0.6782	0.5565	0.5565	-/-
0.35	-	-	-	-	0.7563	0.5644	0.5643	-/-

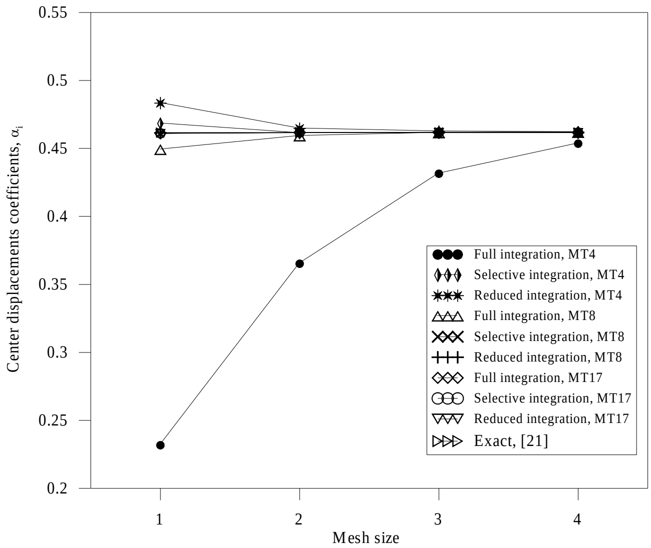

Fig. 6 Center displacement coefficients, αi, of the simply supported square plates for different mesh sizes with t/a=0.10

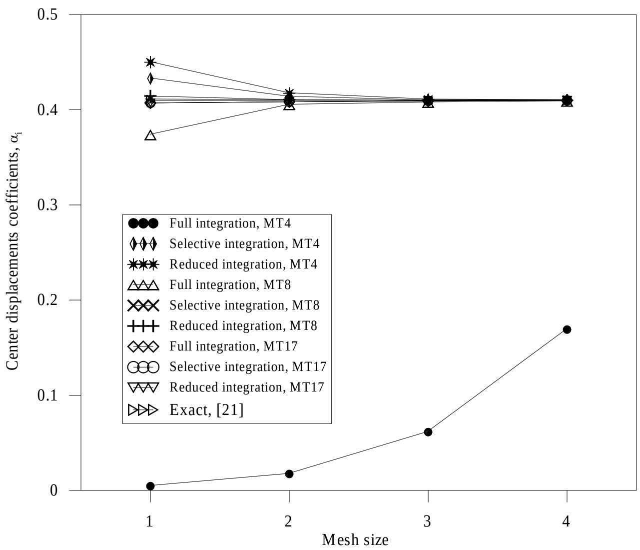

Fig. 7 Center displacement coefficients, αi, of the simply supported square plates for different mesh sizes with t/a=0.01

As seen from Table 7 and Fig. 7, center displacement coefficients, α_i, of the simply supported plates shows locking phenomenon for 0.01, 0.001 t/a ratios with MT4 element. But for 0.01 ratio this locking can be avoiding by increasing mesh size. This solution is not preferred because of wasting time and computer capacities by engineer. For 0.001 ratio there is a little improvement to the locking with increasing mesh size. This ratio needs excessive mesh size than 0.01 ratio for avoiding locking. Writers think that shear locking phenomenon is a mesh problem related with thick plates t/a ratios.

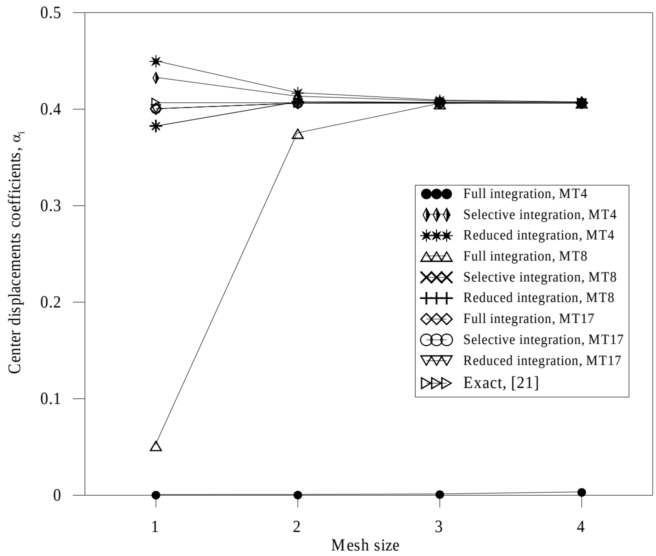

Fig. 8 Center displacement coefficients, αi, of the simply supported square plates for different mesh sizes with *t/a*=0.001

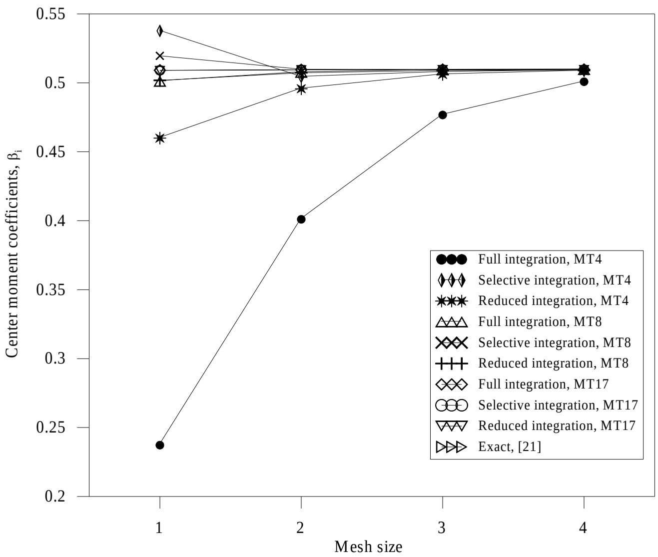

Fig. 9 Center moment coefficients, βi, of the simply supported square plates for different mesh sizes with *t/a*=0.1

As seen from Table 7 and Figs. 8, 9, 10, 11, locking phenomenon occurs always MT4 element with full integration for all *t/a* ratios. Also this problem occurs MT8 element with full integration with 0.001 ratio. Locking phenomenon can be staving off with reduced and selective integration techniques. This can be seen that table and figures. And it can also staving off with using higher order finite elements. This can be also seen that table and figures. MT17 element shows perfect results than MT4 and MT8 element with full integration.

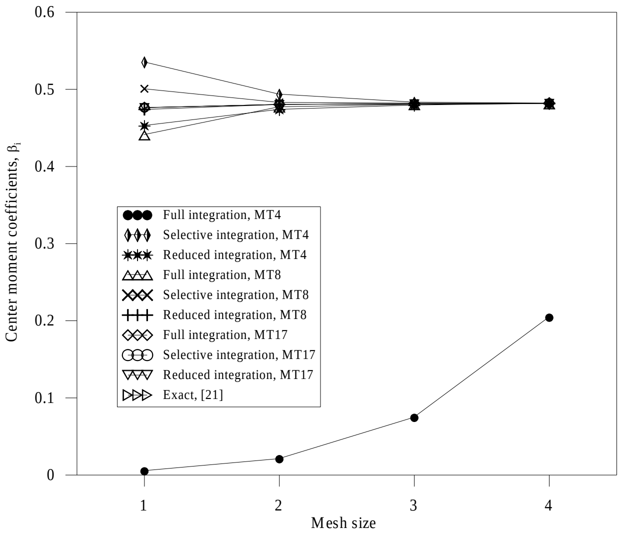

Fig. 10 Center moment coefficients, *βi*, of the simply supported square plates for different mesh sizes with *t/a*=0.01

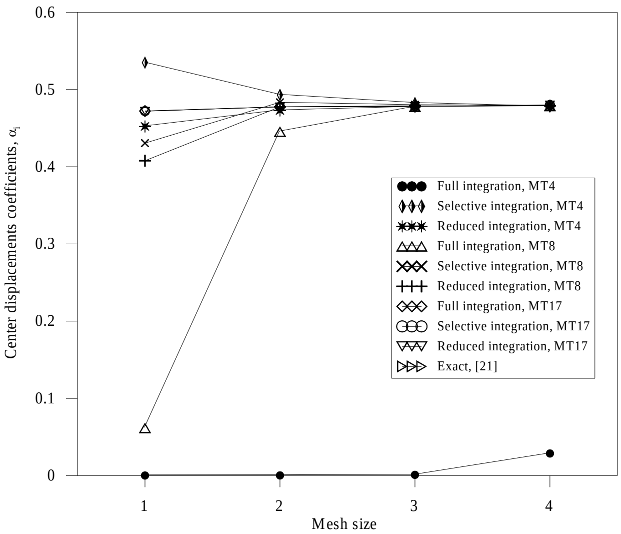

Fig. 11 Center moment coefficients, *βi*, of the simply supported square plates for different mesh sizes with *t/a*=0.001

In general, the results obtained in this study are better than the results given in the literature.

5. Conclusions

In this study, 4-, 8-and 17-noded finite elements are used to obtain the maximum displacements and bending moments of the plates clamped and simply supported along all four edges. The results are compared with the results given in the literature. It is concluded that, by using 17-noded finite element, the mesh size required to produce the desired accuracy can be approximately reduced to the half of those of the others given in the literature. The results obtained by using 17-noded finite element almost coincide with the exact result for 16×16 (256 element) mesh sizes. The results of this study are better than the results given in the literature if they are compared with the exact results. In addition, the following conclusions can be drawn from the results obtained in this study.

• Locking phenomenon is a mesh problem and can be stave off with increasing mesh size.

• If this solution is not preferred then using higher order plate finite element or using integration techniques is a solution for this problem.

• Convergence of the maximum displacement of the plates modeled by 17-noded rectangular finite element is much faster than that of the plates modeled by 8-, and 4-noded rectangular finite element.

References

Bathe, K.J. (1996), *Finite Element Procedures*, Prentice Hall, Upper Saddle River, New Jersey.

Belounar, L. and Guenfoud, M. (2005), "A new rectangular finite element based on the strain approach for plate bending", *Thin Wall. Struct.*, **43**(1), 47-63.

Belytschko, T., Stolarski, B. and Carpenter, N. (1984), "A C0 triangular plate element with one-point quadrature", *Int. J. Numer. Method. Eng.*, **20**, 787-802.

Cen, S., Long, Y., Yao, Z. and Chiew, S. (2006), "Application of the quadrilateral area coordinate method", *Int. J. Numer. Eng.*, **66**, 1-45.

Cook, R.D., Malkus, D.S. and Michael, E.P. (1989), *Concepts and Applications of Finite Element Analysis*, John Wiley & Sons, Inc., Canada.

Çelik, M. (1996), "Plak sonlu elemanlarda kayma şekildeğiştirmelerinin gözönüne alınması ve iki parametreli zemine oturan plakların hesabı için bir yöntem", Ph. D. Thesis, İstanbul Technical University, İstanbul.

Düster, A. (2001), "High order finite elements for three-dimensional thin-walled nonlinear continua", Ph.D. Thesis of Technische Universitat München.

Flanagan, D.P. and Belytscho, T. (1981), "Uniform strain hexahedron and quadrilateral with orthogonal hourglass control", *Int. J. Numer. Method. Eng.*, **17**, 679-706.

Hughes, T.J.R. (2000), *The Finite Element Method*, Dover Publications.

Hughes, T.J.R., Cohen, M. and Harou, M. (1978), "Reduced and selective integration techniques in the finite element analysis of plates", *Nucl. Eng. Des.*, **46**, 203-222.

Hughes, T.J.R., Taylor, R.L. and Kalcjai, W. (1977), "Simple and efficient element for plate bending", *Int. J. Numer. Meth. Eng.*, **11**, 1529-1543.

Ibrahimbegovic, A. (1993), "Quadrilateral finite elements for analysis of thick and thin plates", *Comput. Meth. App. M.*, **110**, 195-209.

Lovadina, C. (1996), "A new class of mixed finite element methods for Reissner-Mindlin Plates", *SIAM J. Numer. Anal.*, **33**, 2457-2467.

Mindlin, R.D. (1951),"I"nfluence of rotatory inertia and shear on flexural motions of isotropic, elastic plates", *J. Appl. M.*, **18**, 31-38.

Olovsson, L., Simonsson, K. and Unosson, M. (2006), "Shear locking reduction in eight-noded tri-linear solid finite elements", *Comput. Struct*., **84**, 476-484.

Owen, D.R.J. and Zienkiewicz, O.C. (1982), "A refined higher-order C^o plate bending element", *Comput. Struct.*, **15**, 83-177.

Ozkul, T.A. and Ture, U. (2004), "The transition from thin plates to moderately thick plates by using finite element analysis and the shear locking problem", *Thin Wall. Struct.*, **42**, 1405-1430.

Özdemir, Y.I., Bekiroğlu, S. and Ayvaz, Y. (2007), "Shear locking-free analysis of thick plates using

Mindlin's theory", *Struct. Eng. Mech*., **27**(3), 311-331.

Özdemir, Y.I. (2007), "Parametric analysis of thick plates subjected to earthquake excitations by using Mindlin's theory", Ph. D. Thesis, Karadeniz Technical University, Trabzon.

Panc, V. (1975), *Theory of Elastic Plates*, Noordhoff, Leidin.

Reissner, E. (1945), "The effect of transverse shear deformation on the bending of elastic plates", *J. Appl. Mech. (ASME)*, **12**, A69-A77.

Reissner, E. (1950), "On a variational theorem in elasticity", *J. Math. Phys.*, **29**, 90-95.

Timoshenko, S. and Woinowsky-Krieger, S. (1959), *Theory of Plates and Shells*, Second Edition, McGraw-Hill., New York.

Soh, A.K., Cen, S., Long, Y. and Long, Z. (2001), "A new twelve DOF quadrilateral element for analysis of thick and thin plates", *Eur. J. Mech., A-Solid.*, **20**, 299-326.

Weaver, W. and Johnston, P.R. (1984), *Finite elements for structural analysis*, Prentice Hall, Englewood Cliffs; New Jersey.

Yuan, F.G. and Miller, RE. (1988), "A rectangular finite element for moderately thick flat plates", *Comput. Struct.*, 30, 1375-87.

Yuan, F-G. and Miller, R.E. (1989), "A cubic triangular finite element for flat plates with shear", *Int. J. Numer. Eng*., **18**(1), 1-15.

Yuqiu, L. and Fei, X. (1992), "A universal method for including shear deformation in thin plates elements", *Int. J. Numer. Eng.*, **34**, 171-177.

Zienkiewich, O.C., Taylor, R.L. and Too, J.M. (1971), "Reduced integration technique in general analysis of plates and shells", *Int. J. Numer. Meth. Eng.*, **3**, 275-290.

Zienkiewicz, O.C., Xu, Z., Ling, F.Z. and Samuelsson, A. (1993), "Linked interpolation for Reissner-Mindlin plate element: part I-a simple quadrilateral", *Int. J. Numer. Meth. Eng.*, **36**, 3043-3056.